IOSR Journal Of Applied Physics (IOSR-JAP)
e-ISSN: 2278-4861.Volume 16, Issue 4 Ser. 1 (July. – August. 2024), PP 26-33
www.Iosrjournals.Org

Comprehensive study on physical and structural properties of $50B_2O_3$-$20Bi_2O_3$-$(30-x)TeO_2$-$xBaO$ glasses

Shaik Rajiya[1*], M.A. Samee[2], Md. Shareefuddin[1], D. Karuna Sagar[1]
1 Department of Physics, University College of Science, Osmania University, Hyderabad 500007, India
2 Department of Physics, University College of Technology, Osmania University, Hyderabad 500007, India

Abstract
Introducing a glass modifier transforms the physical properties of the host glass network. Studying the effects of Ba^{2+} as a glass modifier, various physical and FT-IR experiments were performed on glasses with different compositions of $50B_2O_3$-$20Bi_2O_3$-$(30-x)TeO_2$-$xBaO$ (where x = 5, 10, 15, 20 and 25 mole%). X-ray diffractograms were obtained for glass samples at room temperature. Based on the X-ray diffractograms, it can be concluded that the glass samples lack any distinct peaks, suggesting that they have an amorphous structure. Using the Archimedes principle, the density (ρ) of the glass samples was determined. Physical attributes such as molar volume (V_m) and oxygen packing density (OPD) were measured. Spectral data in the 400–2000 cm^{-1} range were obtained using infrared spectroscopy.

Keywords: *Glasses, Density, Bands in FTIR.*

Date of Submission: 21-07-2024 Date of Acceptance: 31-07-2024

I. Introduction

Tellurite glass is appropriate for photonic applications, nonlinear optical applications, lasers, and communication applications [1]. Because of its good thermal, optical, and electric qualities and stability at room temperature, tellurite glass is frequently used [2, 3]. This glass can be employed in optical amplifiers, non-linear devices, photorefractive materials, and up-conversion lasers because of its high linear and non-linear refractive index and low photon energy [4-6]. Various metal oxides have been incorporated into the tellurite glass system to enhance its optical properties, like Sb_2O_3, Bi_2O_3, Nb_2O_5, MoO_3, etc., [7, 8]. Several authors have carried out numerous investigations on glass based on tertiary tellurite [9–16]. As Tiefeng et al. [14] demonstrated, bismuth dissolution in the tellurite glass matrix enhanced the glass's non-linear properties. This enhancement was directly proportional to the bismuth content and inversely proportional to the barium content. In their study, they explored the optical non-linear properties of TeO_2-Bi_2O_3-BaO glass.

Ceramic materials and optical fibre use bismuth (iii) oxide because it can provide a high refractive index at low temperatures [17]. Its strong polarizability and low field strength valance cation are also useful in the electronic field [18, 19].

The special physical characteristics of tellurites and their industrial significance in producing glasses with desired structural and optical qualities have led to extensive research on boro-tellurite (B_2O_3-TeO_2) glasses. Because boro-tellurite glasses include B_2O_3 and TeO_2, their optical characteristics and structure must be precisely specified for industrial applications [17]. Chemical modifiers like Bi_2O_3 and BaO are added to the glasses to boost their density and enhance their structural and optical qualities.

Barium (BaO), a heavy metal utilized in electro-ceramics and high-temperature conductors, is another safe heavy metal. Barium is not poisonous, does not bioaccumulate, and is not carcinogenic. It is highly helpful in the glass-making industry and can raise the glass's lustre and refractive index [20].

The structure of B_2O_3-TeO_2 glasses is composed of TeO_4 trigonal bipyramidal, TeO_3 pyramidal, BO_4 tetrahedral units, and TeO_3 trigonal units, with an accidentally high B_2O_3 concentration of TeO_6 octahedral [21]. Studying materials' absorption spectra is an essential source of knowledge on the band structure and energy gap. Iskandar and colleagues [22] have examined the optical characteristics of glass containing varying concentrations of Pb-B_2O_3-TeO_2.

When additional glass formers and modifiers are added, the conditional glass formers TeO_2 and Bi_2O_3 are more inclined to form glass. These two materials cannot vitrify on their own under typical circumstances. The bismuth borate glass system's optical characteristics and capacity to produce glasses are improved by adding Ba^{2+} ions with a wide radius and strong polarizability [23, 24]. A literature survey indicates that very little systematic research has been done on bismuth-modified barium boro-tellurite glasses. In this research, we have examined how BaO affects the optical characteristics of bismuth boro-tellurite glasses.

Scientists have studied borate glasses containing heavy metal oxides like bismuth, tellurium, and barium oxide. These glasses have caught their attention due to their unique characteristics, such as high density, low melting temperature, a wide range of glass formation, excellent physical and chemical stability, and interesting nonlinear optical properties [25]. Heavy metal oxides typically do not form glasses independently due to their lower field strength, unlike regular glass-forming oxides. When combined with HMO, bismuth oxide glasses have demonstrated diverse uses in various fields, such as glass ceramics, optoelectronics, γ-ray absorption, mechanical and thermal sensing, and scintillation detection [26].

It is important to remember that, in typical melting circumstances, pure TeO_2 lacks its glassy network. Hence, to produce tellurite-based glasses, it is necessary to use network modifiers or glass-forming oxides. Alkali or alkaline earth oxides, or sometimes a combination of both, can be incorporated into glasses to modify their structural and physical properties. These network modifier oxides disrupt the bridging oxygen bonding in the glass network, generating non-bridging oxygen (NBO) [27].

Accordingly, in terms of glass compositions and melting conditions, high TeO_2-containing glasses can exhibit a range of colours, from vivid purple to light green [28]. With components B_2O_3 and Bi_2O_3, we created a novel series of glass compositions in this study, which is based on barium-modified tellurite glass. In this research, the physical properties of tellurite-based glass were measured in terms of various barium contents. Studies on a tellurite glass system's molar volume and density were ascertained. To investigate the structural alterations of BaO-TeO_2 glasses by adding B_2O_3 and Bi_2O_3 utilizing FTIR spectra.

II. Experimental

Glass preparation

The melt-quenching technique was used to form $50B_2O_3$-$20Bi_2O_3$-(30-x)TeO_2-xBaO glasses with x=5, 10, 15, 20 and 25 mole% of bismuth-boro-tellurite and BaO as a network modifier. The highest purity analytic reagent grade chemicals, TeO_2, Bi_2O_3, and B_2O_3, were used as starting materials and combined in an agate mortar for 20 minutes. After being transferred into porcelain crucibles, the batch materials were heated electrically in a muffle furnace set at 900–950 degrees Celsius until a clear, bubble-free melt was achieved. After a short period, the liquid was transferred onto a stainless-steel plate and placed next to another, both kept at a temperature of 200°C. To reduce thermal stresses in the glass, the glass samples underwent a temperature of 200°C for 12 hours.

Glass characterization

Figure 1 shows XRD patterns of $50B_2O_3$-$20Bi_2O_3$-(30-x)TeO_2-xBaO glasses. All the glass samples lack distinctive peaks, indicating their amorphous nature.

The density (ρ) of the glass samples at room temperature was determined by applying the Archimedes principle and using xylene as the immersion liquid (ρ = 0.86 g/cc). Infrared absorption spectroscopy of the current glasses was performed in the mid-infrared (400–2000 cm^{-1}) range using a Bruker optical spectrometer (Tensor 27, Germany).

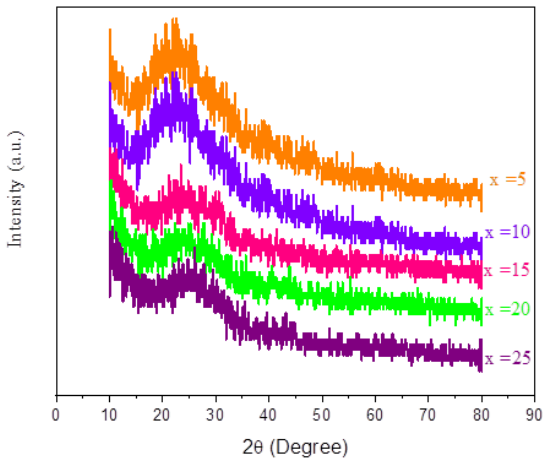

Fig.1. X-ray Diffraction of $50B_2O_3$-$20Bi_2O_3$-(30-x) TeO_2-xBaO (where x= 5, 10, 15, 20 and 25 mole%) glass system.

III. Results And Discussions

Physical properties

The examined glasses' surfaces lack microstructures and display an amorphous phase characteristic, as seen in Fig. 2 in a scanning electron micrograph. Equation (1) was used to determine density using the Archimedes method at room temperature and xylene as the immersion liquid.

$$\rho = \frac{W_A}{W_A - W_L} \times \rho_L \qquad (1)$$

When measuring, the weight of the glass sample in xylene liquid is W_L and in air W_A at room temperature, with the density of xylene being 0.86 g/cc. The measurements were conducted with an extremely high precision, accurate to 0.001 g/cc.

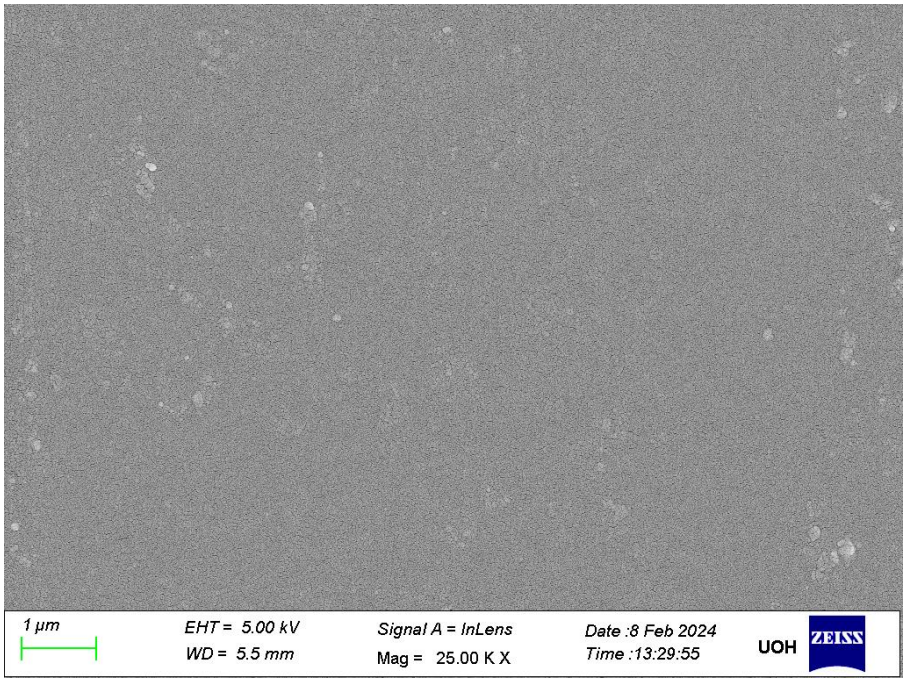

Fig.2. SEM photograph of typical glass sample $50B_2O_3$-$20Bi_2O_3$-$20TeO_2$-10BaO.

The compositional shift changed synthetic glasses' density ρ and molar volume V_m. It shows the impact of the glass structure's hardness, compactness, and toughness [29]. Table 1 presents the molar volume and density data for the synthesized samples. The results show a decrease in the density of the generated samples from 5.76 to 5.52 g/cc, as shown in Fig. 3; also shown in Table 1, the molar volume of the synthesized samples increases from 30.44 to 31.56 cc/mole. The compactness of the glass network structure can significantly influence the range of molar volume values (V_m) [30].

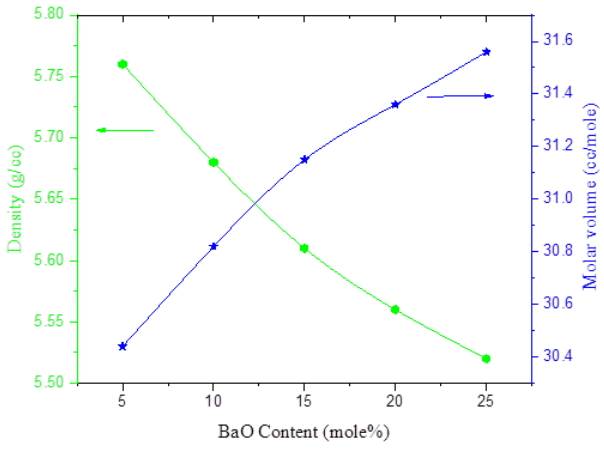

Fig.3. Variation of density and molar volume of present glass system.

Present glasses get less dense as the amount of barium oxide rises. TeO_2's higher density (6.70 g/cc) compared to BaO's (5.72 g/cc) is another factor contributing to the drop in glass density with BaO concentration. According to Table 1, an increase in BaO concentration decreased oxygen packing density from 87.03 to 77.61 (g-atm/cc). However, the oxygen molar volume (V_o) increased from 11.48 to 12.88 (cc/mole). Bi3+ ions (NBi) concentration dropped in the produced glasses as Barium rose. Including BaO in the glasses increased their molar volume, indicating a relaxation in the glass structure. The concentration of BaO is directly connected to the increase in the polaron radius (r_p) and the inter-ionic separation (r_i). The strength surrounding Bi^{3+} ions grew, as indicated by Table 1, decreasing bismuth ion field strength values and increasing boron-boron separation, which were computed using formulae [31].

Table 1. Average molecular weight MW, experimental density ρ, molar volume V_m, oxygen packing density OPD, oxygen molar Volume Vo, Bi^{3+} ion concentration N_{Bi}, polaron radius r_p, inter ionic distance r_i Field strength F_s and boron-boron distance d_{B-B}, theoretical density ρ_{th}, cross-link density $\overline{n}_c$, bond density n_b and co-ordination number of glass m of $50B_2O_3$-$20Bi_2O_3$ -(30-x)TeO_2-xBaO (x = 5, 10, 15, 20 and 25 mole %) glasses.

Physical Parameters	X = 5	X = 10	X = 15	X = 20	X = 25
MW (g/mol)	175.568	175.255	174.941	174.628	174.314
ρ (g/cc)	5.76	5.68	5.61	5.56	5.52
V_m (cc/mol)	30.44	30.82	31.15	31.36	31.56
OPD (g.atm/l)	87.03	84.34	81.86	79.71	77.61
Oxygen molar volume Vo (cc/mol)	11.48	11.85	12.21	12.54	12.88
N_{Bi} (*10^{21} ions/cc)	3.95	3.90	3.86	3.84	3.81
r_p (Å)	2.54	2.55	2.56	2.57	2.58
r_i (Å)	6.32	6.34	6.37	6.38	6.39
Field strength F_s (*10^{16} cm^{-2})	12.78	12.68	12.59	12.53	12.47
V_m^B	30.44	30.82	31.15	31.36	31.56
d_{B-B} (Å^0)	3.69	3.71	3.72	3.73	3.74
ρ_{th} (g/cc)	4.65	4.66	4.67	4.68	4.69
Cross-link Density $\overline{n}_c$	1.94	2.00	2.05	2.11	2.17
Bond density n_b (*10^{22}) (cc^{-1})	8.90	8.98	9.08	9.21	9.34
Coordination no. of glass m	4.5	4.6	4.7	4.8	4.9

FTIR Spectrum

Fourier transform infrared spectroscopy (FTIR) is a highly effective method for obtaining the absorption spectrum of solids, liquids, or gases in the infrared range. Additionally, it can offer some structural hints about the material's overall molecular structure. Figure 4 displays all the boro-tellurite glass systems' infrared spectra with varying additives.

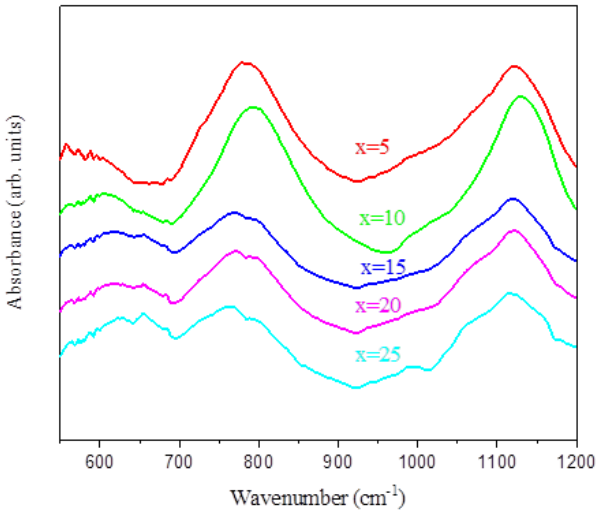

Fig.4 Shows the FTIR spectra of the present glasses.

These spectrums cover the 400–2000 cm^{-1} range. The infrared spectra display multiple broad, moderate-band peaks, as Figure 4(a-e) illustrates. The de-convoluted FTIR spectra's peak locations and amplitudes are presented in Table 2. Due to the chaotic structure, a diffuse band is observed in the 500–600 cm^{-1} range; this represents the vibration modes of the TeO_3 and TeO_4 entities [32].

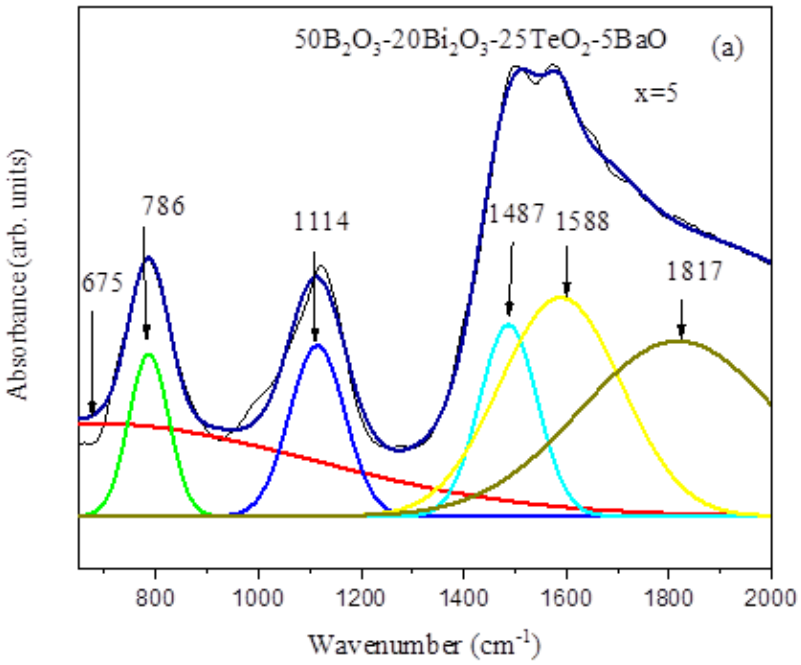

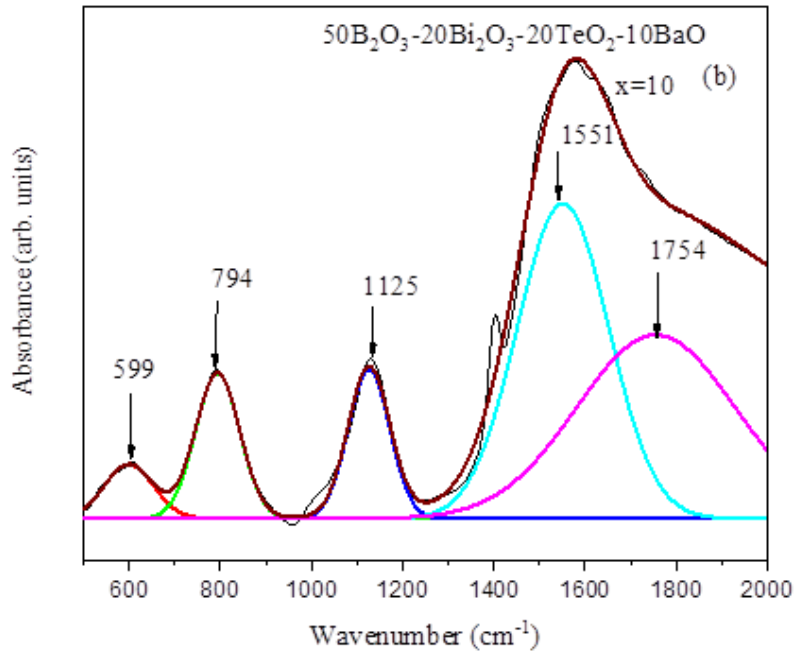

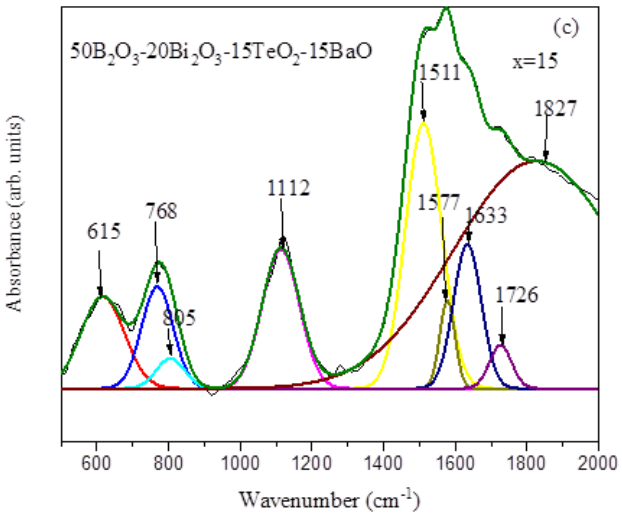

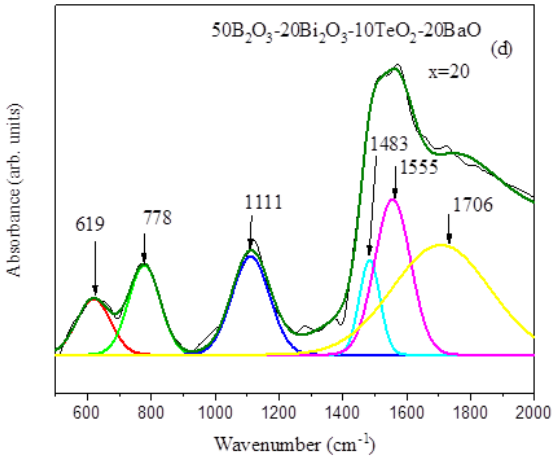

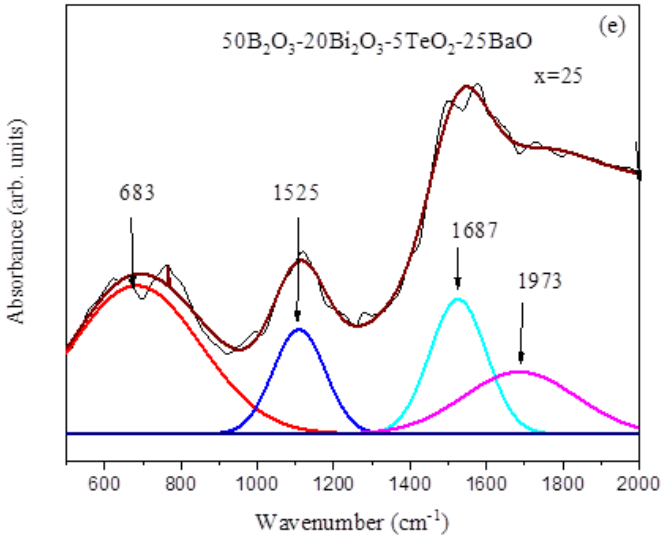

Fig.4 (a-e) Shows deconvoluted FTIR spectra of present glasses.

Bending vibrations of BO_3 triangles: 628-671 cm^{-1} [33]. The huge bands centered at 700 cm^{-1} are composed of band vibration modes in both TeO_{3+1} units, referred to as the tellurium atoms' intermediate coordination between 3 and 4. TeO_4 units and TeO_4 tetrahedrons connected by Te_{ax}-O-Te_{eq} chains have a shoulder at around 775-768 cm^{-1}, which is attributed to the symmetric vibration of Te_{2eq} [34].

In infrared spectra, the six-membered boroxol ring's distinctive peak is 805 cm^{-1} [35]. B-O stretching vibrations in BO_4 units from the Penta, tetra, and tri-borate groups are thought to be responsible for the IR band seen between 1104 and 1110 cm^{-1} [36]. In metaborate, pyroborate, and orthoborate units, the Asymmetric stretching vibrations of the BO3 triangles are responsible for bands between 1335 and 1368 cm^{-1} [37]. Infrared radiation detected in the 1482–1649 cm^{-1} range is ascribed to the stretching vibrations of BO_3 triangles connected to a substantial portion of the borate network [38]. The allocations for the FTIR bands are displayed in Table 3.

Table 2: Peak position (cm^{-1}) and amplitude (A) (a.u) of deconvoluted peaks of FTIR spectra of different compositions of $50B_2O_3$-$20Bi_2O_3$-$(30-x)TeO_2$-xBaO (x= 5, 10, 15, 20 and 25 mole %).

X=5		X=10		X=15		X=20		X=25	
C	A	C	A	C	A	C	A	C	A
		599	794.45	615	896.66	619	762.45		
675	7536.53							683	6536.51
				768	723.79	778	1144.56		
786	1198.35	794	1909.44	805	192.31			1109	1881.39
						1111	1484.67		
				1112	1163.41				
1114	1745.49	1125	1846.93			1483	789.09		
1487	2042.36			1511	2167.24			1525	2620.41
		1551	8590.98			1555	2257.22		
				1577	302.77				
1588	4907.35			1633	904.58			1687	2410.39

Table 3: Assignment of the FTIR Scattering bands measured in $50B_2O_3$-$20Bi_2O_3$-(30-x)TeO_2-xBaO glasses for (x= 5, 10, 15, 20 and 25 mole %).

Wavenumber (cm^{-1})	IR Assignments
500-600 cm^{-1}	Vibration modes of both the TeO_3 and the TeO_4 entities [32]
628-671 cm^{-1}	Vibrations of BO_3 triangles [33]
~700 cm^{-1}	Vibration modes of bonds in both TeO_{3+1} [34]
~775-768 cm^{-1}	Symmetric vibration of Te_{2eq} in TeO_4 units and TeO_4 tetrahedrons linked with Te_{ax}-O-Te_{eq} chains [34]
~805 cm^{-1}	Six membered boroxol ring [35]
1104-1110 cm^{-1}	Penta borate, tetra borate, and tri-borate groups [36]
1335-1368 cm^{-1}	Asymmetric stretching vibrations of the BO_3 triangles in metaborate, pyroborate, and orthoborate units [37]
1482-1649 cm^{-1}	Stretching vibrations of BO_3 triangles attached to large segment of borate network [38]

IV. Conclusions

- From the current work on the physical, optical, and structural properties of $50B_2O_3$-$20Bi_2O_3$-(30-x)TeO_2-xBaO glasses, where x =5, 10, 15, 20, and 25 mole%, the following results have been made.
- The fact that none of the samples had any Bragg's peaks indicated how amorphous they are in XRD Spectra.
- There is a decrease in density and a rise in the molar volume of glass samples as the BaO concentration increases.
- The disordered structure of the material results in a diffuse band in the 500–600 cm^{-1} range, which is thought to represent the vibration modes of both the TeO_3 and TeO_4.
- The huge bands centred at 700 cm^{-1} are composed of bond vibration modes in both TeO_{3+1} units, referred to as the tellurium atoms' intermediate coordination between 3 and 4. A shoulder at around 775-768 cm^{-1} is accredited to the symmetric vibration of Te_{2eq} in TeO_4 units and TeO_4 tetrahedrons connected to Te_{ax}-O-Te_{eq} formula.
- Infrared radiation detected in the 1482–1649 cm^{-1} range is ascribed to the stretching vibrations of BO_3 triangles connected to a substantial portion of the borate network.

Acknowledgments

This research work is gratefully acknowledged to CSIR-NEW DELHI for providing a CSIR-SRF fellowship to one of the authors, Shaik Rajiya, Department of Physics, Osmania University, and also the authors thank the Head, Department of Physics, Osmania University, Hyderabad, for providing the necessary experimental facilities to carry out this work.

Author contributions

All authors contributed to the study conception and design, material preparation, data collection, and analysis.

Funding

The authors declare that no funds, grants, or other support were received during the preparation of this manuscript. Authors Dr. M.A. Samee, Dr. Md Shareefuddin, and Senior Professor D. Karuna Sagar declare they have no financial interests. Author Shaik Rajiya has received a Senior Research Fellowship from CSIR-NEW DELHI.

Declaration of competing interest

The author declares that they have no known competing financial interests or personal relationships that could have appeared to influence the work reported in this paper.

Declarations

Research Data Policy and Data Availability Statement The datasets generated during and analysed during the current study are available from the corresponding author upon reasonable request. Supplemented data: Data will be supplied at a reasonable request.

V. REFERENCES

1. Vijaya Prakash, G.; Narayana Rao, D.; Bhatnagar, A.K. Linear optical properties of niobium-based tellurite glasses. Solid State Commun. 2001, 119, 39–44.

2. Mohamed, N.B.; Yahya, A.K.; Deni, M.S.M.; Mohamed, S.N.; Halimah, M.K.; Sidek, H.A.A. Effects of concurrent TeO_2 reduction and ZnO addition on elastic and structural properties of $(90-x)TeO_2–10Nb_2O_5–(x)ZnO$ glass. J. non-Cryst. Solids 2010, 356, 1626–1630.

3. Foldvari, I.; Peter, A. Basic spectroscopic properties of bismuth tellurium oxide, Bi_2TeO_5. J. Mater. Sci. 1992, 27, 750–754.

4. Udovic, M.; Valant, M.; Suvorov, D. Phase formation and dielectric characterization of the $Bi_2O_3–TeO_2$ system prepared in an oxygen atmosphere. J. Am. Ceram. Soc. 2004, 87, 591–597.

5. Ozdanova, J.; Ticha, H.; Tichy, L. Optical band gap and Raman spectra in some $(Bi_2O_3)x(WO_3)y(TeO_2)100−x−y$ and $(PbO)x(WO_3)y(TeO_2)100−x−y$ glasses. J. non-Cryst. Solids 2009, 355, 2318–2322.

6. Boyer, J.C.; Vetrone, F.; Capobianco, J.A. Optical transitions and upconversion properties of Ho^{3+} doped $ZnO–TeO_2$ glass. J. Appl. Phys. 2003, 93, 9460–9465.

7. Mori, H.; Kitami, T.; Sakata, H. Electrical conductivity of $W_2O_5–Sb_2O_3–TeO_2$ glasses. J. non-Cryst. Solids 1994, 168, 157–166.

8. Szu, S.P.; Chang, F.-S. Impedance study of $V_2O_5–TeO_2–BaO$ glasses. Solid State Ion. 2005, 176, 2695–2699.

9. Ayuni, J.N.; Halimah, M.K.; Talib, Z.A.; Sidek, H.A.A.; Daud, W.M.; Zaidan, A.W.; Khamirul, A.M. Optical properties of ternary $TeO_2–B_2O_3–ZnO$ glass system. Mater. Sci. Eng. 2011, 17.

10. Mohamed, N.B.; Yahya, A.K.; Deni, M.S.M.; Mohamed, S.N.; Halimah, M.K.; Sidek, H.A.A. Effects of concurrent TeO_2 reduction and ZnO addition on elastic and structural Properties of $(90−x)TeO_2–10Nb_2O_5–(x)ZnO$ glass. J. non-Cryst. Solids 2010, 356, 1626–1630.

11. Boris, L.S.; Petrov, T.; Yoneda, H.; Rositsa, T.; Boriana, M. Synthesis and nonlinear optical properties of $TeO_2–Bi_2O_3–GeO_2$ glasses. Scr. Mater. 2009, 61, 493–496.

12. Durga, D.K.; Veeraiah, N. Dielectric dispersion in $ZnF_2–Bi_2O_3–TeO_2$ glass system. J. Mater. Sci. 2001, 36, 5625–5632.

13. Yousef, E.S.S. Characterization of oxyfluoride tellurite glasses through thermal, optical and ultrasonic measurements. J. Phys. D Appl. Phys. 2005, 38, 3970–3975.

14. Xu, T.; Chen, F.; Dai, S.; Shen, X.; Wang, X.; Nie, Q.; Liu, C. Glass formation and third-order optical nonlinear properties within $TeO_2–Bi_2O_3–BaO$ pseudo-ternary system. J. non-Cryst. Solids 2011, 357, 2219–2222

15. Senthil Murugan, G.; Fargin, E.; Rodriguez, V.; Adamietz, F.; Couzi, M.; Buffeteau, T.; Le Coustumer, P. Temperature-assisted electrical poling of TeO_2–Bi_2O_3–ZnO glasses for non-linear optical application. J. non-Cryst. Solids 2004, 344, 158–166.

16. Wang, Y.; Dai, S.; Chen, F.; Xu, T.; Nie, Q. Physical properties and optical band gap of new tellurite glasses within the TeO_2–Nb_2O_5–Bi_2O_3 system. Mater. Chem. Phys. 2009, 113, 407–411.

17. El-Mallawany, R.A.H. Tellurite Glasses Handbook; CRC Press Inc.: Boca Raton, FL, USA, 2002.

18. El-Mallawanny, R.; Dirar Abdalla, M.; Abbas Ahmed, I. New tellurite glass: Optical properties. Mater. Chem. Phys. 2008, 109, 291–296.

19. Hooi Ming Oo, Halimah Mohamed-Kamari and Wan Mohd Daud Wan-Yusoff, Optical Properties of Bismuth Tellurite Based Glass, Int. J. Mol. Sci. 2012, 13, 4623-4631.

20. A.Azuraida, M.K. Halimah, A.A. Sidek, C.A.C. Azurahanim, S.M. Iskandar, M. Ishak, A. Nurazlin, Comparative studies of bismuth and barium boro-tellurite glass system: structural and optical properties, Chalcogenide Letters, Vol. 12, No. 10, October 2015, p. 497 – 503.

21. S. Rada, M. Culea and E. Culea, Journal of Non-Crystalline Solids, 354, 5491 (2008).

22. S. M. Iskandar, M. K. Halimah, W. M. Daud, H. A. A. Sidek, and A. R. Azhar, Int. J. Mol. Sci., 14, 3201 (2013).

23. S. Dhankhar, R. S. Kundu, S. Rani, P. Sharma, S. Murugavel, R. Punia and N. Kishore, Electron Mater. Lett. 13, 412-419 (2017).

24. Sunita Rani, R. S. Kundu, Neetu Ahlawat, Suman Rani, Kanta Maan Sangwan, Kanika Rani, Bismuth Modified Physical and Optical Properties of Barium Boro-Tellurite Glasses, DAE Solid State Physics Symposium 2018 AIP Conf. Proc. 2115, 030255-1–030255-4.

25. E. Culea, L. Pop, P. Pascuta, M. Bosca 2009 J. Mol. Struct. 924 192.

26. A. Agarwal, V.P. Seth, P.S. Gahlot, S. Khasa, P. Chand 2003 J. Phys. Chem. Solids. 64 2281.

27. B Srinivas, Abdul Hameed, M N Chary and Md Shareefuddin, Physical, Optical and FT-IR studies of Bismuth-Boro-tellurite Glasses containing BaO as modifier, IOP Conf. Series: Materials Science and Engineering 360 (2018) 012022.

28. Penprapa Punpai and Shigeki Morimoto, Structure and properties of TeO_2- containing borate glasses, Suranaree J. Sci. Technol. 16(1):47-51.

29. H.A. Abo-Mosallam, E.A. Mahdy, Synthesis and characterization of sodium calcium

Fluorophosphates glasses containing MoO_3 for potential use in sealing applications, J. Non-Crystalline Solids 546 (2020), 120279.

30. Sidek, H.A.A.; Rosmawati, S.; Talib, Z.A.; Halimah, M.K.; Daud, W.M. Synthesis and optical properties of ZnO–TeO_2 glass system. Am. J. Appl. Sci. 2009, 6, 1489–1494.

31. Shaik Rajiya, M. A. Samee, Md. Shareefuddin, D. Karuna Sagar, An investigation on physical, thermal, linear, non-linear optical and structural properties of (70-x)B_2O_3-10ZnO-10CdO-10BaO-xBi_2O_3 glasses, Applied Physics A (2024) 130:43.

32. Munoz-Matin, D.; Villegas, M.A.; Gonzalo, J.; Fernandez-Navarro, J.M. Characterisation of glasses in the TeO_2–WO_3–PbO system. J. Eur. Ceram. Soc. 2009, 29, 2903–2913.

33. Kirti Nanda, Neelam Berwal, R.S. Kundu, R. Punia, N. Kishore, Effect of doping of Nd^{3+} ions in BaO–TeO_2–B_2O_3 glasses: A vibrational and optical study, Journal of Molecular Structure 1088 (2015) 147–154.

34. Tiefeng Xu , Feifei Chen, Shixun Dai, Xiang Shen, Xunsi Wang , Qiuhua Nie , Chao Liu, Kai Xu, Jong Heo, Glass formation and third-order optical nonlinear properties within TeO_2–Bi_2O_3–BaO pseudo-ternary system, Journal of Non-Crystalline Solids 357 (2011) 2219–2222.

35. E.I. Kamitsos, M.A. Karakassides, G.D. Chryssikos, A vibrational study of lithium sulfate based fast ionic conducting borate glasses, J. Phys. Chem. 90 (1986) 4528–4533.

36. E.I. Kamitsos, M.A. Karakassides, G.D. Chryssikos, Vibrational spectra of magnesium-sodium-borate glasses. 2. Raman and mid-infrared investigation of the network structure, J. Phys. Chem. 91 (1987) 1073.

37. S. Arunkumar, K. Marimuthu, concentration effect of Sm^{3+} ions in B_2O_3–PbO–PbF_2–Bi_2O_3–ZnO glasses-structural and luminescence investigations, J. Alloys Compd. 565 (2013) 104–114.

38. L. Singh, V. Thakur, R. Punia, R.S. Kundu, A. Singh, Structural and optical properties of

barium titanate modified bismuth borate glasses, Solid State Sci. 37 (2014) 64–71.